

Chapter 10

Application and Control of Quadrotors



Safanah M. Raafat, Firas A. Raheem, Ahmed A. Alawsi,
and Zainab S. Mahmood

Abstract A quadrotor is a multirotor helicopter, boosted by four rotors. In contrast to fixed-wing aircraft, quadrotors are categorized as rotorcraft, since their lift is produced by a set of rotors. The usage of quadrotors has increased in recent years in civilian and military operations. They are adaptable during vertical takeoff and landing and have stability when hovering. Additionally, quadrotors have low power consumption and are unobtrusive.

The many important applications of quadrotors include delivery and monitoring. A quadrotor can fly in an autonomous and non-autonomous manner with use of methods using the proportional integral derivative (PID) and linear quadratic regulator (LQR), sliding mode control, and fuzzy control. Such methods stabilize the quadrotor through flights. The aim of most controllers is to eliminate the error which is the difference between a measured value (measured states by sensors) and a desired set-point (desired states). The “error” can be minimized by adjusting the control inputs and the speed of the motors, in an iterative manner. This chapter illustrates key applications, and further the modeling and control of quadrotors is described in brief. Two cases of studies are presented, the first of which deals with the design of PID control for precise positioning of delivery quadrotors, and the second entails the design of multiple model adaptive control (MMAC) of the quadrotor.

Key words Quadrotor · Multirotor · Delivery · Power consumption · PID · MMAC

S. M. Raafat (✉)

Automation and Robotics Research Unit, Control and Systems Engineering Department,
University of Technology-Iraq, Baghdad, Iraq
e-mail: 60154@uotechnology.edu.iq

F. A. Raheem · Z. S. Mahmood

Control and Systems Engineering Department, University of Technology-Iraq, Baghdad, Iraq
e-mail: 60124@uotechnology.edu.iq; zainabalsafar299@gmail.com

A. A. Alawsi

College of Science, Physics Department, University of Wasit, Wasit, Iraq
e-mail: aalawsi@uowasit.edu.iq

10.1 Introduction

The study of micro unmanned air vehicles (UAVs) through developing technologies enables expansive application. UAVs are useful in a wide array of operations and have gained importance. UAVs are aircraft which may be flown without a pilot (Newcome 2004).

Modern rotorcraft UAVs have many benefits compared to old-styled crafts, including improved maneuverability, an ability to fly above objectives, and capacity to take off and land in limited space in comparison to fixed-wing crafts. Quadrotors belong to the class of rotorcrafts and are recognized by their simple structure, ease of maintenance, and unsophisticated dynamics in comparison to those of helicopters (Schmidt 2011).

Quadcopters operate in two flight modes: autonomous and non-autonomous. Non-autonomous flights are controlled by the user through a radio device (control joystick) as shown in Fig. 10.1.

In autonomous flight, the quadcopter flies and controls itself, carrying out required missions without user interference. Quadcopters operate with a global positioning system (GPS) sensor to ascertain their linear position in relation to other sensors and achieve a stable and balanced flight. The GPS sensor connects with GPS satellite systems as shown in Fig. 10.2 and uses information provided for operation (Grisso et al. 2009; Rahemi et al. 2014; Ziaul 2016).

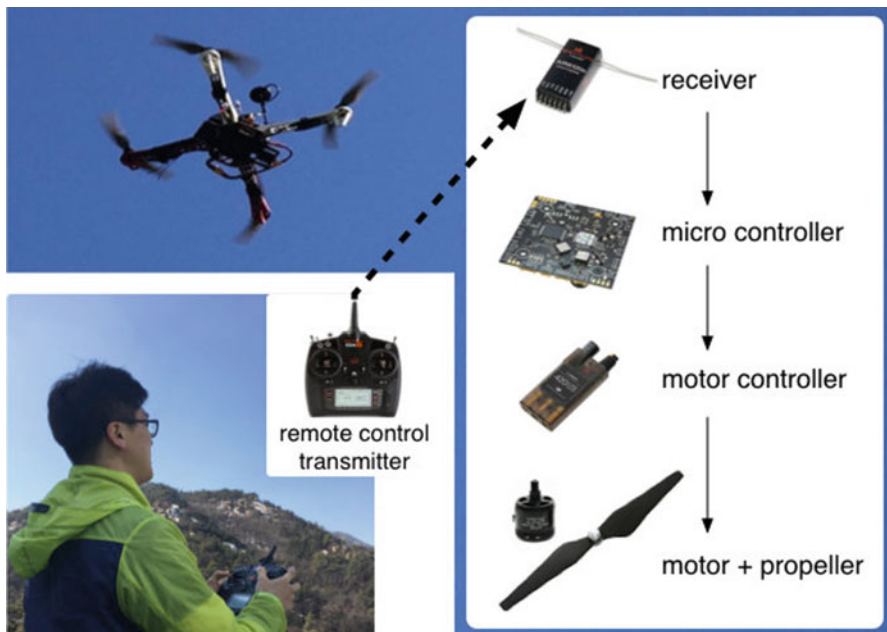


Fig. 10.1 Joystick control of a quadcopter through non-autonomous flight (Jung et al. 2018)

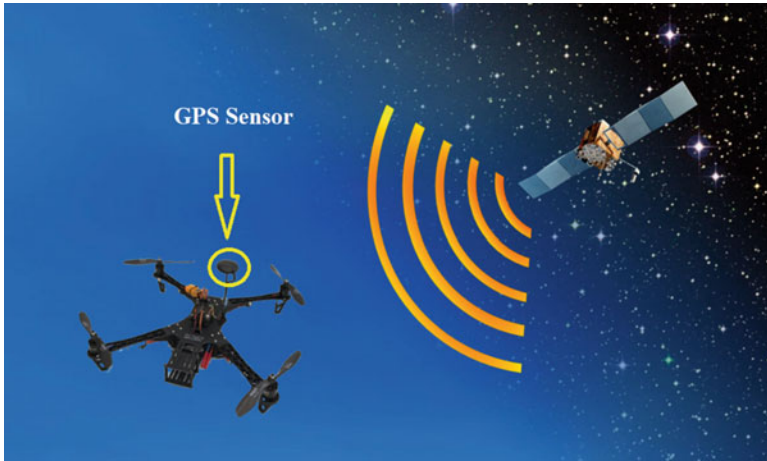


Fig. 10.2 Quadcopters control themselves in autonomous flight using a Global Positioning System (GPS)

In the literature, the many types of control methods applied in autonomous or non-autonomous modes include PID (Ferry 2017), LQR (Purnawan et al. 2017), sliding mode (Tripathi et al. 2016; Thomas 2010), fuzzy control (Sattar and Ismail 2017), image recognition (Luo et al. 2016), and adaptive control (Minh et al. 2014), stabilizing and improving their flight performance.

The remaining parts of this chapter are structured as follows: Sect. 10.2 details applications of quadrotor UAVs; Sect. 10.3 presents the modeling of a (six degrees of freedom) quadrotor; Sect. 10.4 discusses quadrotor control; and Sect. 10.5 features two case studies of quadrotor control, the first case demonstrates the design of a PID controller for delivery quadrotor systems and the second shows the design of a Multiple Model Adaptive Control (MMAC) based on three Kalman filters (KFs). Conclusions and prospective future directions are covered in Sect. 10.6.

10.2 Applications of Quadrotors

Common quadrotor applications (Air Drone Craze, Drone Deals 2019) are detailed in this section.

10.2.1 Journalism, Filming, and Aerial Photography

Quadcopters are increasingly popular in photography of sport events, competitions, and cinematography owed to their maneuverability, takeoff, and vertical landing, as

well as hovering. Drones have recently started to be used in the direct broadcasting of satellite channels by linking live broadcast cameras to Earth stations, which in turn are transmitted through the satellite channel.

10.2.2 Shipping/Delivery

One of the most important properties of quadrotors is their ability to be operated autonomously through a range of techniques. Avoiding traffic and jammed roads, UAVs are used to deliver small parcels, letters, medicines, and even pizzas over short distances.

10.2.3 Disaster Management, Search, and Rescue/Healthcare

The task of rescuing people exposed to hazards or perilous circumstances at night and in difficult terrain is a race against time. Equipped with thermal cameras, quadcopters can be used to locate people and rapidly assess situations.

10.2.4 Geographic Mapping

The ability of the quadcopter to reach/overview uneven terrain enables its use in the collection of accurate information with high-precision cameras for geographic mapping.

10.2.5 Structural Safety Inspections

The quadcopter is used by various sectors to provide accurate assessment, such as in checking building structures, electric power lines, and crude oil pipelines. Increased visual clarity and thermal, water, and gaseous sensors allow identification of potential future problems, in order that one may take appropriate measures to prevent them from happening.

10.2.6 Precision Agriculture

Quadcopters help farmers to closely monitor agricultural fields, enabling them to improve management and increase production. Quadcopters are additionally used in

spraying pesticides, covering vast areas in a fast and consistent manner, with improved coverage while losses of pesticides are reduced.

10.2.7 Wildlife Monitoring/Poaching

The quadcopter assists security services charged with protection of remote, wild areas by detecting hunters trapping rare animals, often useful where extinction is a very present threat. They may also be used to detect the positions of sick animals more quickly allowing necessary actions to be carried out to help and preserve them.

10.2.8 Law-Enforcement and Border Patrol

The quadcopter assists the police and security services in law enforcement operations, especially in preventing the smuggling of drugs and prohibited substances by monitoring external and internal borders of countries.

10.2.9 Construction Sites

Quadcopters help to provide three-dimensional vision of construction stages, thus enabling engineers to detect errors early for process and increased safety of projects.

10.2.10 Entertainment

Plenty of hobbyists are picking up quadrotors to play around with, both in remote flight and by programming quadrotor AI (artificial-intelligence). As such quadrotors can be used in many ways to capture videos and photographs.

10.2.11 Military and Law Enforcement

The quadcopter is used extensively in military fields today to carry out multiple tasks including reconnaissance and surveillance of enemy sites (Armed Quadrotors Are Coming 2014). For example, a small UAV may be used in provision of visual surveillance of a drug trafficker's compound deep in the jungle (Dhanalakshmi et al. 2015).

10.3 Modeling of Quadrotors

Generally, a quadcopter is characterized by four independently controllable actuators (motors) assembled in a cross configuration as shown in Fig. 10.3. The actuators are two clockwise (CW) and two counterclockwise (CCW), so the affected rotational torque on the body around the Z axis of the quadcopter is cancelled during the hovering state (Allen 2014; Quadcopter 2017; Fernando et al. 2013). The figure shows two basic coordinate frames called inertial frames, being a fixed earth frame and body frame. The two frames are used to identify the quadrotor's locations and attitude in order that translation and rotation matrices can be applied to transfer the vehicle from one coordinate frame to another (Fernando et al. 2013; Alaiwi and Mutlu 2018).

In this section, the performance of unmanned rotorcraft is demonstrated using a six degree of freedom (6-DoF) prototype model. The quadrotor includes four propellers responsible for lift force. Propellers are driven by four motors that are fixed onto a frame with a plus shape structure. Dynamic modeling is usually developed using the Newton Euler Formula, where the drive force and produced torque are regarded as the main quadrotor control elements (Magnussen and Skjonhaug 2011).

Quadrotor control is taken into consideration as a multivariable and as a substitute nonlinear system due to its dynamics, having sturdy coupling among translation and angular motion, and suffers from external disturbances related to flight surroundings and the effect of huge payload variability. These factors demand a robust control design. The control goal is to allow for sudden changes and rewards an ability of

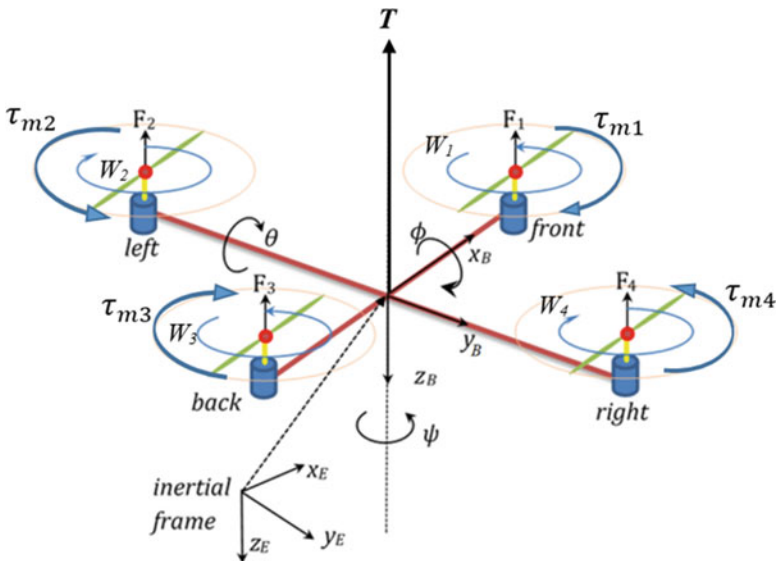


Fig. 10.3 The inertial and body frames of a quadrotor

discovering improved tracking performance in contrast to any modeling error and uncertainty.

The quadrotor has a linear position $\xi = (x, y, z)$ and the attitude (angular position) defined by Euler angles $H = (\text{roll } (\phi), \text{pitch } (\theta), \text{yaw } (\psi))$ with respect to the inertial frame. The Euler angles determine the rotation of the quadrotor around each axis ($x, y,$ and z axis, respectively). The roll angle determines rotation around the x -axis, while the pitch angle determines rotation around the y axis and the yaw angle determines rotation around the z -axis. The angular velocity in the body frame $V = [p, q, r]$ can be related to the Euler angles velocities $(\dot{x}, \dot{y}, \dot{z})$ in the same frame by the following relation:

$$V = W_H \dot{\theta}$$

$$\begin{bmatrix} p \\ q \\ r \end{bmatrix} = \begin{bmatrix} 1 & 0 & -s_\theta \\ 0 & c_\phi & c_\theta s_\phi \\ 0 & -s_\phi & c_\theta s_\phi \end{bmatrix} \begin{bmatrix} \dot{\phi} \\ \dot{\theta} \\ \dot{\psi} \end{bmatrix} \quad (10.1)$$

where $c_\phi = \cos(\phi)$, $s_\phi = \sin(\phi)$, $c_\theta = \cos(\theta)$, $s_\theta = \sin(\theta)$, and W_H is the transformation matrix for angular velocities from the inertial frame to the body frame. Conversely, a rotation matrix (R) can be used to transform the linear velocity ($\eta = [u \ v \ w]$) from the body frame to the inertial frame. The matrix R has an orthogonal property, so $R^T = R^{-1}$ (Castillo–Zamora et al. 2018; Bouzgou et al. 2017; Gordon et al. 2016).

$$R = \begin{bmatrix} c_\psi c_\theta & c_\psi s_\theta s_\phi - s_\psi c_\phi & c_\psi s_\theta c_\phi + s_\psi s_\phi \\ s_\psi c_\theta & s_\psi s_\theta s_\phi + c_\psi c_\phi & s_\psi s_\theta c_\phi - c_\psi s_\phi \\ -s_\theta & c_\theta s_\phi & c_\theta c_\phi \end{bmatrix} \quad (10.2)$$

The quadrotor has four motors which are used to provide it with the required thrust force (T), moving in the direction of the body z -axis. These are calculated via (10.3) and (10.4) as

$$T = \sum_{i=1}^4 T_i = k(w_1^2 + w_2^2 + w_3^2 + w_4^2) \quad (10.3)$$

$$T_i = f_i = k w_i^2 \quad (10.4)$$

where T_i is the thrust force generated by the i th motor, k is the thrust factor, and w_i is the angular velocity of the i th motor. The motors provide the quadcopter with required torques τ_ϕ , τ_θ , and τ_ψ in the direction corresponding to the body frame (Alaiwi and Mutlu 2018; Bouzgou et al. 2017). This is further expanded in (10.5) as follows:

$$\tau_B = \begin{bmatrix} \tau_\phi \\ \tau_\theta \\ \tau_\psi \end{bmatrix} = \begin{bmatrix} lk(-w_2^2 + w_4^2) \\ lk(-w_1^2 + w_3^2) \\ k(w_2^2 + w_4^2 - w_1^2 - w_3^2) \end{bmatrix} = \begin{bmatrix} IU_2 \\ IU_3 \\ U_4 \end{bmatrix} \quad (10.5)$$

where l is the distance from the centre of the motor to the center of mass of the quadrotor; U_2 , U_3 , and U_4 are input forces to the quadrotor generated by motors. These forces can be calculated as

$$U_2 = f_2 - f_4 = k(-w_2^2 + w_4^2) \quad (10.6)$$

$$U_3 = f_1 - f_3 = k(-w_1^2 + w_3^2) \quad (10.7)$$

$$U_4 = f_2 + f_4 - f_1 - f_3 = k(w_2^2 + w_4^2 - w_1^2 - w_3^2) \quad (10.8)$$

Each motor generates an extra torque τ_{m_i} around its rotor axis which can be calculated by

$$\tau_{m_i} = dw_i^2 + I_m \dot{w}_i \quad (10.9)$$

where d , \dot{w}_i , and I_m represent the drag factor, the angular acceleration of the i th motor, and the inertia moment retrospectively. Generally, \dot{w}_i is very small and can be omitted, leading to (10.10)

$$\tau_{m_i} = dw_i^2 \quad (10.10)$$

The quadrotor is assumed to be symmetric, so its inertia matrix I is diagonal with $I_{xx} = I_{yy}$. The inertia matrix of quadcopter around three axes can be represented as

$$I = \begin{bmatrix} I_{xx} & 0 & 0 \\ 0 & I_{yy} & 0 \\ 0 & 0 & I_{zz} \end{bmatrix} \quad (10.11)$$

The linear acceleration ($\ddot{x}, \ddot{y}, \ddot{z}$) and angular acceleration ($\ddot{\phi}, \ddot{\theta}, \ddot{\psi}$) equations are used to represent the dynamic motion equations of the quadrotor. These functions can be derived by Euler-Lagrange equations of motion and Eqs. (10.1, 10.2, 10.3, 10.4, 10.5, 10.6, 10.7, 10.8, 10.9, 10.10, and 10.11) shown above.

The Lagrange equation variable \mathfrak{L} is key in derivation of linear and angular acceleration equations. The Lagrange equation represents the algebraic sum of translational (E_{trans}), rotational (E_{rot}), and potential (E_{pot}) energies. It can be defined as (Alaiwi and Mutlu 2018)

$$\mathfrak{L}(o, \dot{p}) = E_{trans} + E_{rot} + E_{pot} = \frac{m}{2} \dot{\xi}^T \dot{\xi} + \frac{1}{2} v^T I v - mgz \quad (10.12)$$

where $o = \begin{bmatrix} \xi \\ H \end{bmatrix} = [x, y, z, \phi, \theta, \psi]^T$.

Quadcopters are exposed to external forces such as wind that affect the copter's torques. The relationship between external forces and torques can be represented by the following:

$$\begin{bmatrix} f \\ \tau \end{bmatrix} = \frac{d}{dt} \left(\frac{\partial L}{\partial \dot{\sigma}} \right) - \frac{\partial L}{\partial \sigma} \quad (10.13)$$

Linear and angular components are not independent so should be studied separately. Therefore, the linear Euler-Lagrange equations are

$$f = RT^B = m \ddot{\xi} + mg \begin{bmatrix} 0 \\ 0 \\ 1 \end{bmatrix} \quad (10.14)$$

where T^B is the thrust force vector in the direction of body axis and $T^B = [0 \ 0 \ T]^T$. Therefore,

$$\ddot{\xi} = \frac{R}{m} \begin{bmatrix} 0 \\ 0 \\ T \end{bmatrix} - g \begin{bmatrix} 0 \\ 0 \\ 1 \end{bmatrix} \quad (10.15)$$

Equation (10.2) is substituted in Eq. (10.15) to get the following:

$$\begin{bmatrix} \ddot{x} \\ \ddot{y} \\ \ddot{z} \end{bmatrix} = \frac{T}{m} \begin{bmatrix} c_\psi s_\theta c_\phi + s_\psi s_\phi \\ s_\psi s_\theta c_\phi - c_\psi s_\phi \\ c_\theta c_\phi \end{bmatrix} - g \begin{bmatrix} 0 \\ 0 \\ 1 \end{bmatrix} \quad (10.16)$$

As we mentioned earlier, the symbol T represents the thrust force generated by motors. We will replace it with U_1 to format all symbols that represent the forces generated by quadcopter's motors.

$$\left. \begin{aligned} \ddot{x} &= \frac{U_1}{m} (c_\psi s_\theta c_\phi + s_\psi s_\phi) \\ \ddot{y} &= \frac{U_1}{m} (s_\psi s_\theta c_\phi - c_\psi s_\phi) \\ \ddot{z} &= \frac{U_1}{m} c_\theta c_\phi - g \end{aligned} \right\} \quad (10.17)$$

where m represents the mass of the quadrotor.

The relations between angular velocity of motors w_i and generated forces U_1 , U_2 , U_3 , and U_4 by motors can be presented in a matrix form (Armah et al. 2016; Herrera and Gómez 2015).

$$\begin{bmatrix} w_1^2 \\ w_2^2 \\ w_3^2 \\ w_4^2 \end{bmatrix} = \begin{bmatrix} \frac{1}{4k} & 0 & \frac{-1}{2k} & \frac{-1}{4d} \\ \frac{1}{4k} & \frac{-1}{2k} & 0 & \frac{1}{4d} \\ \frac{1}{4k} & 0 & \frac{1}{2k} & \frac{-1}{4d} \\ \frac{1}{4k} & \frac{1}{2k} & 0 & \frac{1}{4d} \end{bmatrix} \begin{bmatrix} U_1 \\ U_2 \\ U_3 \\ U_4 \end{bmatrix} \tag{10.18}$$

The angular Euler-Lagrange equations can be defined as follows:

$$\tau_B = J\ddot{H} + C(H, \dot{H})\dot{H} \tag{10.19}$$

where J is the Jacobian matrix transform from V to \dot{H} and can be defined as follows:

$$\begin{aligned} J &= W_H^T I W_H \\ &= \begin{bmatrix} I_{xx} & 0 & -I_{xx}s\theta \\ 0 & I_{yy}c_\phi^2 + I_{zz}s_\phi^2 & (I_{yy} - I_{zz})c_\phi s_\phi c\theta \\ -I_{xx}s\theta & (I_{yy} - I_{zz})c_\phi s_\phi c\theta & I_{xx}s_\theta^2 + I_{yy}s_\phi^2 c_\theta^2 + I_{zz}c_\phi^2 c_\theta^2 \end{bmatrix} \end{aligned} \tag{10.20}$$

where the c matrix is the Coriolis term containing the gyroscope and centripetal terms (Herrera and Gómez 2015).

Now, Eq. (10.19) can be used to derive angular acceleration equations to get

$$\ddot{H} = J^{-1}(\tau_B - C(H, \dot{H})\dot{H}) \tag{10.21}$$

Then, calculate the inverse of J and substitute it in Eq. (10.21) to get the following angular acceleration equations of the quadcopter:

$$\left. \begin{aligned} \ddot{\phi} &= \frac{I_y - I_z}{I_x} \dot{\theta} \dot{\psi} - \frac{J_r}{I_x} W_r \dot{\theta} + \frac{U_2}{I_x} \\ \ddot{\theta} &= \frac{I_z - I_x}{I_y} \dot{\phi} \dot{\psi} - \frac{J_r}{I_y} W_r \dot{\phi} + \frac{U_3}{I_y} \\ \ddot{\psi} &= \frac{I_x - I_y}{I_z} \dot{\theta} \dot{\phi} + \frac{U_4}{I_z} \end{aligned} \right\} \tag{10.22}$$

where W_r is the algebraic sum of the angular speeds of motors:

$$W_r = -w_1 + w_2 - w_3 + w_4 \tag{10.23}$$

J_r is the inertia of the motor and is a very small value and often can be omitted so Eq. (10.22) and (10.24):

$$\left. \begin{aligned} \ddot{\phi} &= \frac{I_y - I_z}{I_x} \dot{\theta} \dot{\psi} + \frac{U_2}{I_x} \\ \ddot{\theta} &= \frac{I_z - I_x}{I_y} \dot{\phi} \dot{\psi} + \frac{U_3}{I_y} \\ \ddot{\psi} &= \frac{I_x - I_y}{I_z} \dot{\theta} \dot{\phi} + \frac{U_4}{I_z} \end{aligned} \right\} \quad (10.24)$$

Equations (10.17) and (10.24) represent linear and angular motions of quadrotors. The mathematical model can be implemented in MATLAB/Simulink or another environment to perform the tests in multiple scenarios and additional purposes by researchers to achieve optimal performance (Armah et al. 2016).

Linear and angular velocity states can be calculated by integrating Eqs. (10.17) and (10.24), respectively; in turn, linear and angular position states can be calculated by double integration of Eqs. (10.17) and (10.24). The 12 states $(x, \dot{x}, y, \dot{y}, z, \dot{z}, \phi, \dot{\phi}, \theta, \dot{\theta}, \psi, \dot{\psi})$ are the required states for the control of the quadrotor. Some of these states can be measured by sensors, while others can be estimated by special “observers” such as KFs or extended Kalman filters (EKFs).

10.4 Control of Quadrotors

Every type of aircraft has actuators that are used to generate linear and angular forces which enable movement in different ways to achieve the desired position. As mentioned earlier, quadrotors use four motors (actuators) to generate forces but are unable to achieve desired positions without the use of control systems which generate appropriate control signals.

A flight controller is essentially a circuit board with sensors that relays variation in coordinates of the quadrotor. It may receive user commands and controls the rotor’s motors so as to retain the sought after position.

Most control systems reduce the error ratio between desired and sensor-measured signals to generate appropriate control signals for motors, until the quadrotor reaches the desired location where the error signal will be zero. Quadrotors require a highly nonlinear multivariable system that has strong coupling between translation and angular motion and hence are highly sensitive to external disturbances. Moreover, large payload variation may have noticeable effects. Accordingly, robust controller is needed to deal with sudden changes as well as provision of tracking performance in the presence of modeling error and uncertainties. The most commonly used types of controllers are as follows:

Proportional Integral Derivative (PID) Controllers

Different types of PID controllers are usually designed to reach a desired position. However, tuning methods are required to obtain suitable controller settings; for this purpose, Bouabdallah et al. (2004), Pounds et al. (2010), and Argentim et al. (2013) utilized integral time absolute error (ITAE) criteria. In Abbasi et al. (2013), a fuzzy

self-tuned PID controller was proposed. Bergkvist (2013) implemented a PID controller for real-time “Android” operating systems. Sadeghzadeh et al. (2014) implemented single PID and gain scheduling-PID. Kader et al. (2014) proposed PID and compared it with fuzzy controllers for attitude and altitude signals. It is simple to design a PID; it provides good performance and requires minimal control effort. Wang et al. (2016) provided a robust cascade PID controller that alleviates disturbances, and Ferry (2017) designed a PID.

Optimal and Adaptive Controllers

Linear quadratic (LQ) control was applied by Bouabdallah et al. (2004), and a classic linear quadratic regulator (LQR) controller was utilized by Argentim et al. (2013); Araar and Aouf (2014) designed an LQ-servo controller that provides improved performance and attains robust trajectory design even in presence of gusts of wind. Moness and Bakr (2015) and Purnawan et al. (2017) introduced a further LQR controller design for quadrotors.

Adaptive Control

Adaptive control is an advanced control technique to maintain a desired level of control system performance, when the parameters of the plant dynamic model are unknown and/or change in time (Minh et al. 2014).

Nonlinear and Intelligent Controllers

Dikmen et al. (2009) applied different types of nonlinear controllers for quadrotor control systems including inverse dynamic control, feedback linearization control, and sliding mode control. Sliding mode (Thomas 2010; Balasubramanian and Vasantharaj 2013) applied computed torque control mechanism to nonlinear dynamics of a quadrotor with consideration of disturbance; in the latter, improved robustness is gained in the presence of small changes in the payload as compared to other techniques. Yacine et al. (2015) used a combination of a fuzzy logic control (FLC) and a sliding mode control (SMC) in order to improve performance of quadrotors. Sliding mode has been further advanced (Tripathi et al. 2016; Abdullah and Sabar 2015) establishing a fuzzy controller to regulate the height, roll, pitch, and yaw of the quadrotor using a genetic algorithm (GA). In addition, fuzzy control has been applied by Sattar and Ismail (2017).

10.5 Case Studies

10.5.1 Precise Positioning for Delivery Quadrotor

In this case study, the PID control algorithm will be applied to control the position of a quadrotor system. The block diagram used to calculate the PID is shown in Fig. 10.4. The PID is the part of the flight control software that receives the data from sensors and determines the necessary speed of the quadrotor’s motor. There are three parameters in a PID controller, the P , I , and D terms (Liang 2018):

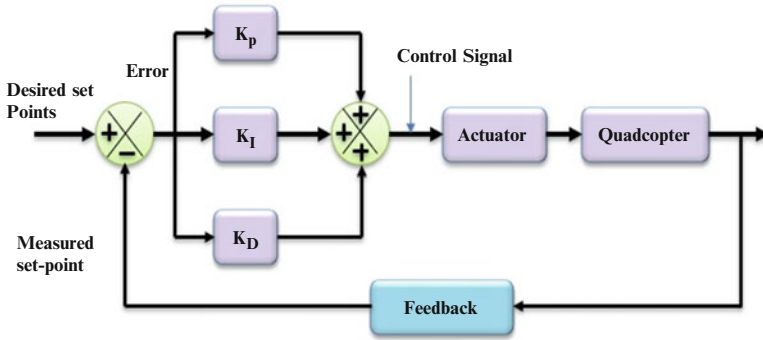


Fig. 10.4 Block diagram of quadcopter control by PID control

- “P” tends to reduce the present error.
- “D” is a prediction of future errors – it helps to accelerate approaching a set-point and counteracts P when it is getting close to minimize overshoot.
- “I” is the accumulation of past errors; it works on reducing the steady-state error by managing the forces that happen over time; for example, if a quad constantly drifts away from a set-point due to wind, it will spool motors up to counteract it.

The general formula of a PID controller (Fernando et al. 2013; Kotarski et al. 2016) can be written as

$$PID(e) = k_p e(t) + k_i \int_0^t e(\tau) d\tau + k_d \frac{d}{dt} \text{state} \tag{10.25}$$

where $e(t) = \text{desired state}(t) - \text{measured state}(t)$, k_p , k_i , and k_d are the proportional, integral, and derivative gains, respectively.

Altitude Control

Appropriate thrust force, U_1 , is required to achieve the desired altitude and can be calculated by

$$U_1 = k_{p_z} e_z + k_{I_z} \int e_z + k_{D_z} \frac{d}{dt} e_z + mg \tag{10.26}$$

where k_{p_z} , k_{I_z} , and k_{D_z} are the altitude PID gains controller; e_z is the altitude error $e_z = z_{des} - z_{meas}$, z_{des} and z_{meas} are desired and measured altitude, respectively; and g is the Earth gravity.

The roll control, pitch control, and yaw control Eqs. (10.27–10.29) are used to determine appropriate torques to achieve the desired attitude.

Roll Control

The following equation is used to determine appropriate torque (U_2) to rotate a quadrotor around the x -axis:

$$U_2 = k_{p_\phi} e_\phi + k_{I_\phi} \int e_\phi + k_{D_\phi} \frac{d}{dt} e_\phi \quad (10.27)$$

where k_{p_ϕ} , k_{I_ϕ} , and k_{D_ϕ} are the roll angle PID gains controller; e_ϕ is the roll angle error; $e_\phi = \phi_{\text{des}} - \phi_{\text{meas}}$; ϕ_{des} and ϕ_{meas} are the desired and measured roll angle, respectively.

Pitch Control

The torque (U_3) is required to rotate a quadrotor around the y -axis and can be calculated by

$$U_3 = k_{p_\theta} e_\theta + k_{I_\theta} \int e_\theta + k_{D_\theta} \frac{d}{dt} e_\theta \quad (10.28)$$

where k_{p_θ} , k_{I_θ} , and k_{D_θ} are the pitch angle PID gains controller; e_θ is the pitch angle error $e_\theta = \theta_{\text{des}} - \theta_{\text{meas}}$; θ_{des} and θ_{meas} are the desired and measured pitch angle, respectively.

Yaw Control

The torque (U_4) is needed to rotate a quadrotor around z -axis and can be properly calculated by

$$U_4 = k_{p_\psi} e_\psi + k_{I_\psi} \int e_\psi + k_{D_\psi} \frac{d}{dt} e_\psi \quad (10.29)$$

where k_{p_ψ} , k_{I_ψ} , and k_{D_ψ} are yaw angle PID gains controller; e_ψ is yaw angle error $e_\psi = \psi_{\text{des}} - \psi_{\text{meas}}$; ψ_{des} and ψ_{meas} are desired and measured yaw angle, respectively.

The current quadrotor model has six DOF and only four actuators (motors), so direct control of all DOF is complex. Meanwhile, the control Eqs. (10.26–10.29) are used to directly control four of the DOF (z , ϕ , θ , ψ). The roll and pitch angles move the quadrotor towards the desired x and y location. Consequently, the desired x and y will be used first to calculate the desired roll and pitch angles in order to control x and y positions indirectly. Meanwhile, the equations that are used to calculate desired roll and pitch angles are obtained in terms of desired x and y as Shahid et al. (2016):

$$\phi_d = \tan^{-1} \left(\frac{U_y \cos \theta_d}{g - U1} \right) \quad (10.30)$$

and

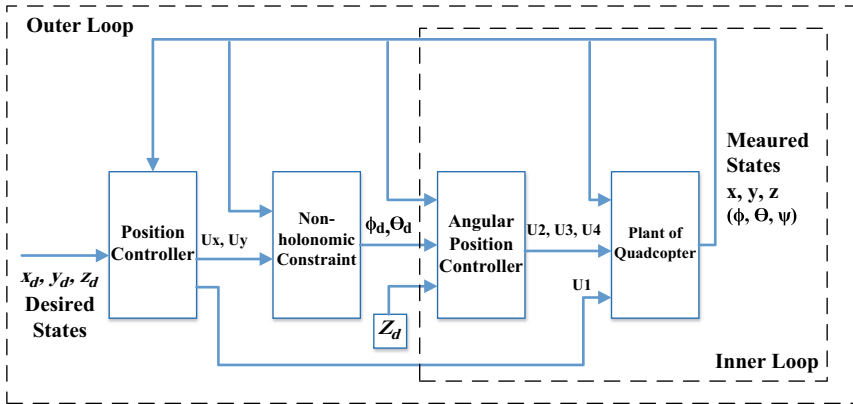


Fig. 10.5 Control block diagram of quadrotor

$$\theta_d = \tan^{-1} \left(\frac{U_x}{U_1 - g} \right) \tag{10.31}$$

where U_x and U_y are calculated as follows:

$$U_x = k_{p_x} e_x + k_{I_x} \int e_x + k_{D_x} \frac{d}{dt} e_x \tag{10.32}$$

$$U_y = k_{p_y} e_y + k_{I_y} \int e_y + k_{D_y} \frac{d}{dt} e_y \tag{10.33}$$

where $e_x = x_{des} - x_{meas}$ is the error position in the direction of x -axis, x_{des} and x_{meas} are desired and measured position in the direction of x -axis, respectively. Further, $e_y = y_{des} - y_{meas}$ is the error position in the direction of y -axis, y_{des} and y_{meas} are the desired and measured position in the direction of the y -axis, respectively.

There are two main control loops: *inner* and *outer*. The outer loop is used to calculate U_1, U_x, U_y, ϕ_d , and θ_d . The inner loop is used to calculate the desired control signals U_2, U_3 , and U_4 . Figure 10.5 shows the overall control block diagram of quadrotor. Control signals U_1, U_2, U_3 , and U_4 are feed to the Electronic Speed Control (ESC) devices to generate appropriate electrical signal used to control the speed of each motor. The block diagram in Fig. 10.5 has been implemented by the technical computing platform Matlab. Figure 10.6a–e shows the simulation response of the states X, Y, Z, ϕ , and θ of the quadrotor under a PID controller for fixed position ($x = 20, y = 15, z = 10$, and $\psi = 0$).

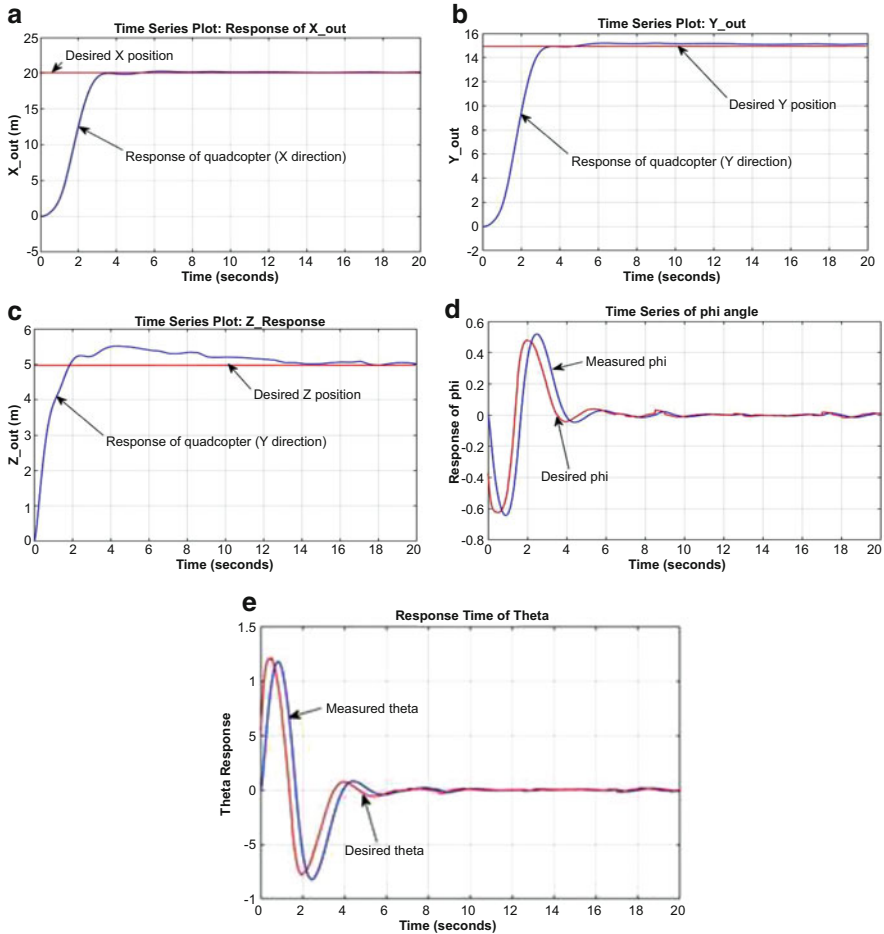


Fig. 10.6 State simulation time response of quadrotor: (a) X-out response; (b) Y-out response; (c) Z response; (d) ϕ response; (e) θ response

10.5.2 Adaptive Positioning of Quadrotor

Multiple model adaptive control (MMAC) is a state feedback controller. This adaptive control implants its construction in a bank of filters as Kalman filters (KFs). For the quadrotor, each KF is intended for an explicit value of payload variation. Then, accordingly, a set of LQ-servo state feedback controllers are designed for tracking reference trajectories. The integral term of the LQ-Servo can effectively eliminate the tracking error.

MMAC is applied here to meet stability and performance requirements in two situations: additive payload, which leads to performance degradation or instability, and fluctuating of the operating point. The appropriate control signal is correlated

with the highest weighting signal in order to provide the required control action. The assigned weighting signals rely on two important elements: the residual and covariance matrices of the KFs. Note that each KF is designed for a model that corresponds to the known value of the uncertain parameter (Hassani et al. 2011; Hassani et al. 2009).

The MMAC comprises of (i) N weighting signal, P_N , that generated from a dynamic weighting signal generator and (ii) a bank of N continuous-time estimator, KF_N . Each estimator is intended for one of the selected adopted models. Each of these carefully chosen models belongs to the original set of the plant's model (Fekri et al. 2006).

The uncertain parameters' vector signifies the uncertainty in linear state model of the quadrotor dynamic system. These parameters tolerate the matrices that define the structure of the linear model. For flexible illustration, it is presumed that the uncertain parameter (a) can take only one value for each run.

The dynamic weights characterize the finest deduction of model that is most likely to be accurate. These weights are supposed be the characterized issue in multiple model algorithms, and they are usually evaluated online. The dynamic weighting is initially set to $1/N$ and fulfils the following condition:

$$(P_i(t)) \in (0, 1) \text{ For } i = 1 \dots N \quad (10.34)$$

The dynamic weights are produced by dynamic weighting signal generator (DWSG) which is denoted by the following differential equation:

$$\dot{P}_i(t) = -\mu \left(1 - \frac{\beta_i(t) e^{-w_i(t)}}{\sum_{j=1}^N P_j(t) \beta_j(t) e^{-w_j(t)}} \right) P_i(t) \quad (10.35)$$

where μ is a positive constant theoretically equals to one and the function $\beta_i(t)$ is denoted by

$$\beta_i(t) = \frac{1}{\sqrt{\det S_i(t)}} \quad (10.36)$$

and $w_i(t)$ is an error measuring function between the measurement states of the quadrotor and the estimated measurable states of each local estimator. It can be evaluated as follows:

$$w_i(t) = \frac{1}{2} \|z(t) - \hat{y}_i(t)\|_2 S_i^{-1}(t) \quad (10.37)$$

$$S_i = C s_i C^T + R_i \quad (10.38)$$

where $s_i(t)$ is a uniformly positive definite weighting matrix, described by

$$\|x\|_2 \mathbf{S} = (x^T \mathbf{S} x)^{(1/2)} \tag{10.39}$$

Each control signal is obtained from the product of the state estimation KF $\hat{x}_k(t|t), k = 1, 2, 3, \dots N$ and the gain supplied by an optimal linear quadratic control, G_k , as

$$u_k(t) = -G_k \hat{x}_k(t|t), k = 1, 2, 3, \dots N \tag{10.40}$$

The ‘‘global’’ control signal, which enters both the quadrotor system and the banks of KFs, is calculated by the probabilistic weighting of each local control signal (Hassani et al. 2009). Consequently, the mixing of state estimation and generated feedback control can be clearly noticed. Therefore, any estimation errors of the state will directly affect the local control signals. Accordingly, in the MMAC design, the identification system and the control system are not separated (Fekri et al. 2007).

The employed MMAC with three KFs is shown in Fig. 10.7. The (a) value equals 0, 0.3, and 0.8 kg for KF number 1, 2, and 3, respectively. The three KFs are run in parallel when the parameter (a) is allocated to the reference model. The three KFs are initialized with $x_o = [2 \ 0 \ 3 \ 0 \ -10 \ 0 \ 0.2 \ 0.3 \ 0 \ 0.05]^T$ values with the initial weighting signal uniformly distributed $P_o = 1/3$ (Raafat and Mahmoud 2018). Figure 10.8 shows the progress with time for the conditional probabilities for the three KFs. The quadrotor system tracks the desired references in about 5 s. This demonstrates the capability of the MMAC of reasonably fast convergence.

Figure 10.9 shows the closed loop responses of MMAC using three KFs, where the model and filters start at the same initial point. Figure 10.9a shows the response of the linear position (x) by using MMAC, where (curve 1) represents the actual response from the model, the estimated signal is represented in (curve 2), and the reference signal is explained in (curve 3). Figure 10.9(a–e) also shows the tracking for $y, z, \text{roll, pitch, and yaw}$, respectively. In Fig. 10.9, the linear and angular positions track the references, and the adaptation of this algorithm can be seen clearly where the actual response follows the true value by adjusting its parameter (a). Accordingly, Fig. 10.10 demonstrates the performance of the MMAC controlled system to follow the applied references. That reflects the capability of the controller to select the correct control signal. The root mean square error (RMSE) is used as a performance index.

Figure 10.11 demonstrates the capability of tracking with initial conditions of the reference model which are different from those of filters which have a value of $x = [5 \ 0 \ 6 \ 0 \ -5 \ 0.1 \ 0 \ 0.3 \ 0.9 \ 0]$. The four motors in our example provide plenty of power for the rotors to climb rapidly. Each motor is designed for ‘aeroplanes’ weighing (280–400 g). For additive payload, we use a large motor that provides more thrust with the same size of propellers. These motors have larger output wattage which usually handles bigger loads sufficiently.

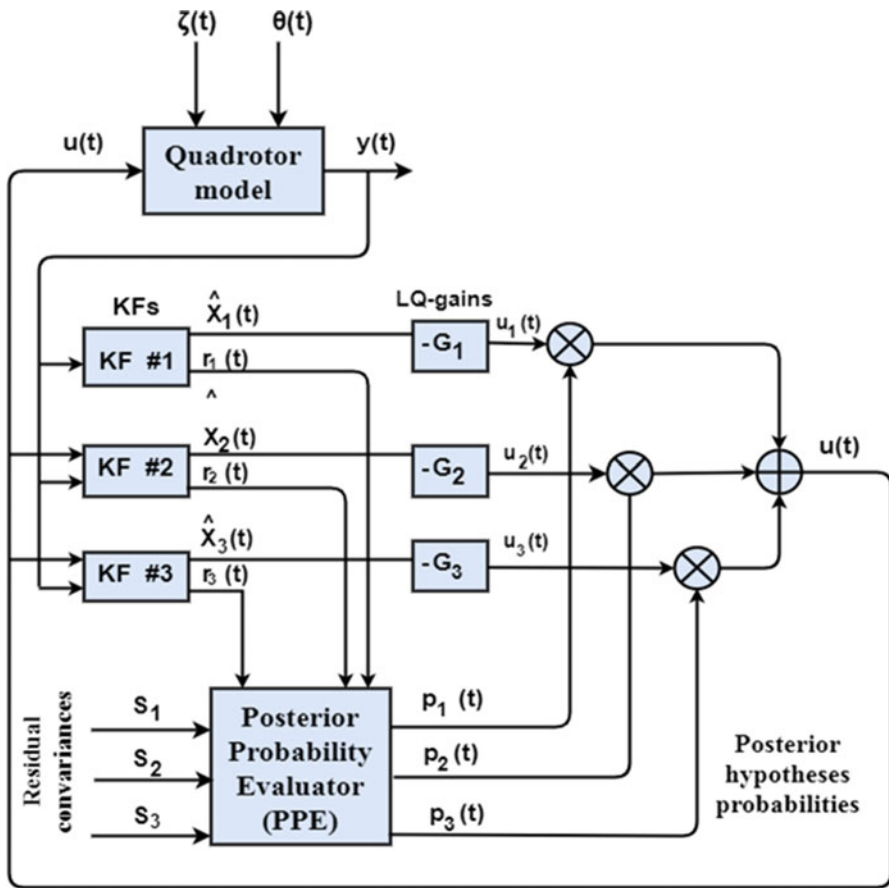


Fig. 10.7 Block diagram of MMAC

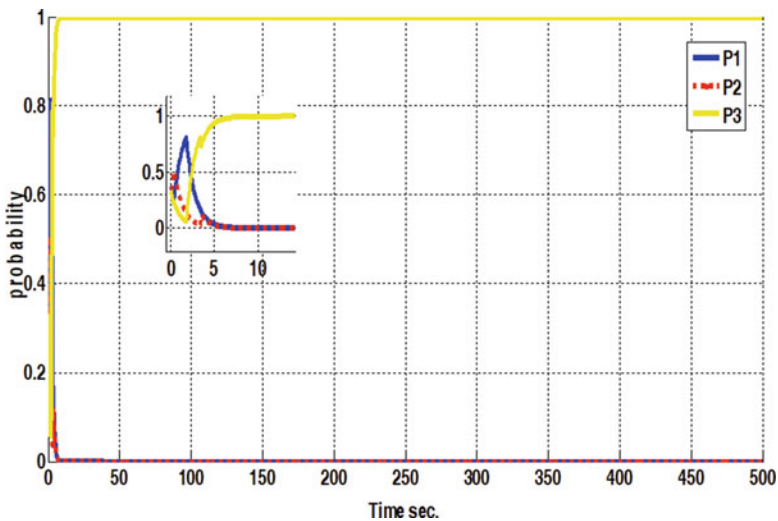


Fig. 10.8 Time histories for probability when the uncertainty in mass of a reference model is 0.8Kg

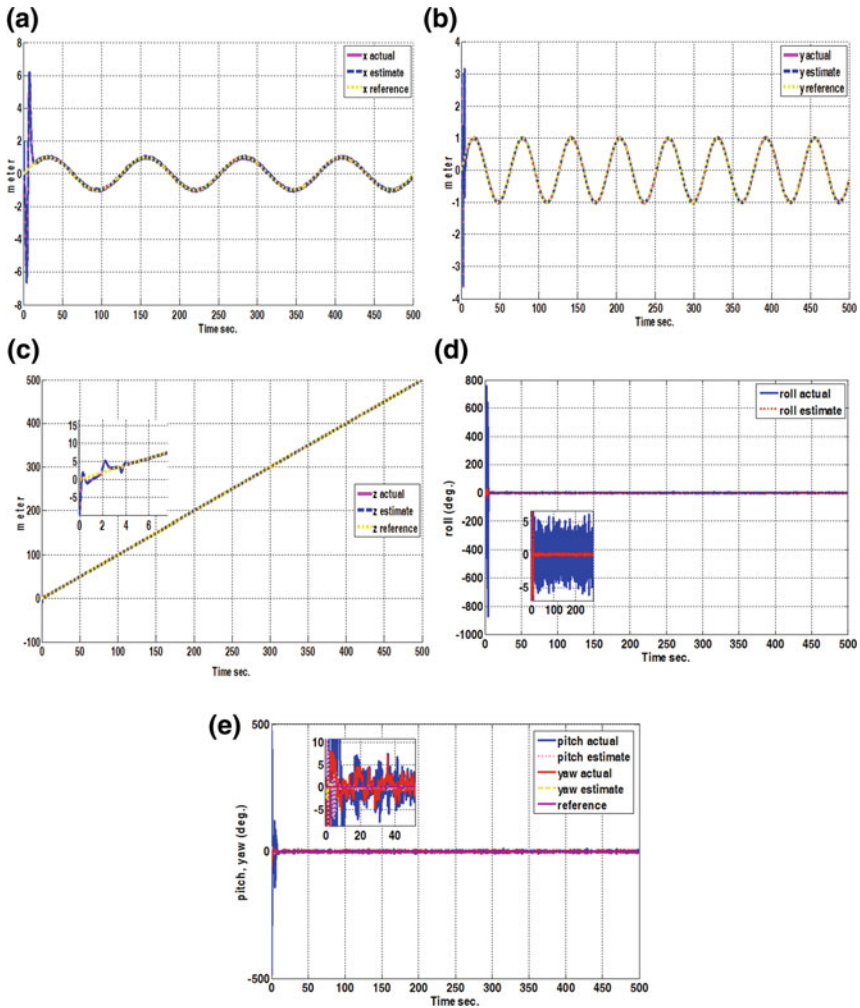


Fig. 10.9 A closed loop response of the reference model for (a) the linear position x ; (b) the linear position y ; (c) the linear position z ; (d) the angular position roll; (e) the angular positions pitch and yaw

10.6 Conclusion and Future Applications

Different types of quadrotors are increasingly used for different applications. The type and application affects the design of the required controller. A high level of safety and reliability need to be assured for social and airspace applications. Accurate measurements are necessary for robust behavior of quadrotors. In order to achieve observability of all the states, it is necessary to use estimators of KFs or EKFs.

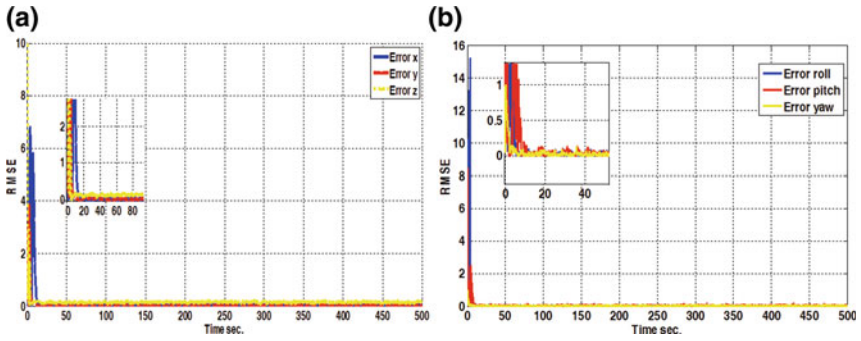


Fig. 10.10 RMSE of tracking design when the mass uncertainty at reference model = 0.8 kg for: (a) The linear position, (b) the angular position

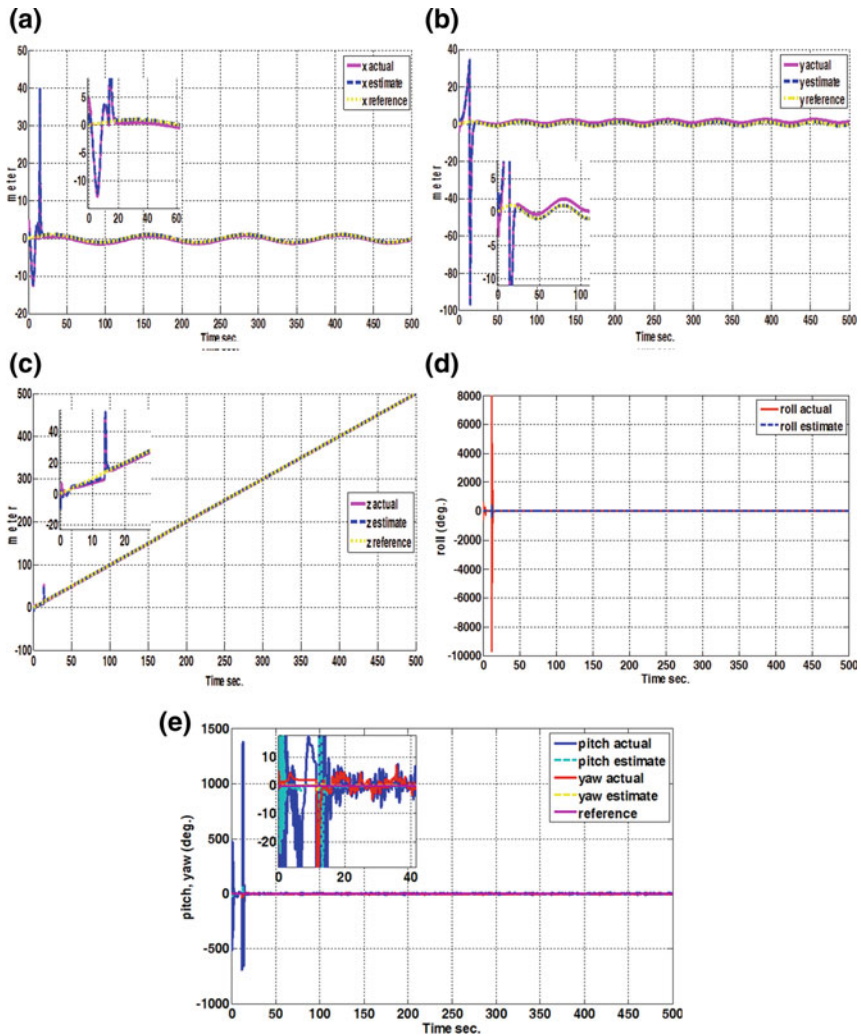


Fig. 10.11 A closed loop response of quadrotor controlled system using MMAC, with Kalman filters (KFs) starting at different initial points from that of the reference model: (a) the linear position x; (b) the linear position y; (c) the linear position z; (d) the angular position roll; (e) the angular position pitch and yaw

Quadrotor has been increasingly used for delivery owed to the low cost, efficiency, and speed of parcel carriage; it overcomes the flow, congestion of roads, and traffic lights. Another important point is the reduction of the pollution of the environment; no combustible fuel is used, and power is supplied via a rechargeable battery. Quadrotors are unobtrusive and may reach rugged areas where cars or other forms of carriage cannot.

In this chapter, two cases of designing a controller for quadrotors have been described. The first presents the development of a PID controller to solve impulse input signal and prevent the system from saturation as well, as well as operating with minimal power under a simple and efficient algorithm. The second case presents the design of MMAC, in which the reference position is effectively tracked. The robustness of the adaptive controller is demonstrated when different initial positions are used from the true initial condition of the quadrotor. The performance of the adaptive control has been evaluated using the RMSE index, demonstrating its robust potential application in resource flow, as part of efficient systematic management of the needs of increasing, potentially remote/variable demographic populations.

References

- Abbasi E, Mahjoob M, Yazdanpanah R (2013) Controlling of quadrotor UAV using a fuzzy system for tuning the PID gains in hovering mode. In: 10th Int Conf Adv Computer Entertain Tech, pp 1–6
- Abdullah F, Sabar RA (2015) Design and implementation of autopilot system for quadcopter. *Int J Sci Eng Comput Technol* 5(6):190–199
- Air Drone Craze, Drone Deals + Information + Resources (2019). Accessed 2019. <https://airdronecraze.com/drones-action-top-12-non-military-uses/>
- Alaiwi Y, Mutlu A (2018) Modelling, simulation, and implementation of autonomous unmanned quadrotor. *Mach Technol Mater* 12(8):320–325
- Allen C (2014) How a quadcopter works. University of Alaska. Available via http://ffden2.phys.uaf.edu/webproj/212_spring_2014/Clay_Allen/clay_allen/works.html. Accessed 27 Oct 2020
- Araar O, Aouf N (2014) Full linear control of a quadrotor UAV, LQ vs H_∞ . In: IEEE, UKACC International Conference on Control (CONTROL). pp 133–138. <https://doi.org/10.1109/CONTROL.2014.6915128>
- Argentim LM, Rezende WC, Santos PE et al (2013) PID, LQR and LQR-PID on a quadcopter platform. In: IEEE, International Conference on Informatics, Electronics & Vision (ICIEV). pp 1–6. <https://doi.org/10.1109/ICIEV.2013.6572698>
- Armah S, Yi Sun, Choi W et al (2016) Feedback control of quad-rotors with a Matlab-based simulator. *Am J Appl Sci* 13(6):779–793. <https://doi.org/10.3844/ajassp.2016.779.793>
- Armed Quadrotors Are Coming (2014) Hearst Magazine Media, Popular Mechanics. <https://www.popularmechanics.com/military/a7926/armed-quadrotors-are-coming-10720086/>. Accessed 27 Oct 2020
- Balasubramanian E, Vasantharaj R (2013) Dynamic modeling and control of quad rotor. *Int J Eng Technol* 5(1):63–69
- Bergkvist H (2013) Quadcopter control using android based sensing. M.Sc. Thesis, Department of Automatic Control, University of Lund

- Bouabdallah S, Noth A, Siegwart R (2004) PID vs LQ control techniques applied to an indoor micro quadrotor. In: IEEE/RSJ, International Conference on Intelligent Robots and Systems (IROS), vol 3. pp 2451–2456
- Bouzgou K, Bestaoui Y, Benchikh L et al (2017) Dynamic modeling, simulation and PID controller of unmanned aerial vehicle UAV. In: The Seventh International Conference on Innovative Computing, Technology. <https://doi.org/10.1109/INTECH.2017.8102445>
- Castillo–Zamora JJ, Camarillo–Gomez KA, Perez–Soto GI et al (2018) Comparison of PD, PID and sliding-mode position controllers for V–tail quadcopter stability. *IEEE Access* 6:38086–38096
- Dhanalakshmi KS, Karthika S, Saravanakumar P et al (2015) Implementation of highly automated UAV with GPS for product delivery using Labview. *Int J Adv Electron Comput Sci* 2(11): 39–42
- Dikmen IC, Arisoy A, Temeltas H (2009) Attitude control of a quadrotor. In: IEEE, 4th international conference on recent advances in space technologies. RAST'09, pp 722–727
- Fekri S, Athans M, Pascoal A (2006) Issues, progress and new results in robust adaptive control. *Int J Adapt Control Signal Process* 20(10):519–579. <https://doi.org/10.1002/acs.912>
- Fekri S, Athans M, Pascoal A (2007) Robust multiple model adaptive control (RMMAC): a case study. *Int J Adapt Control Signal Process* 21(1):1–30. <https://doi.org/10.1002/acs.944>
- Fernando HCTE, De Silva ATA, De Zoysa MDC et al (2013) Modelling, simulation and implementation of a quadrotor UAV. In: IEEE 8th international conference on industrial and information systems, ICIIS, Sri Lanka. <https://doi.org/10.1109/ICIInfS.2013.6731982>
- Ferry N (2017) Quadcopter plant model and control system development with MATLAB/Simulink implementation. M.Sc. Thesis. Rochester Institute of Technology, Rochester
- Gordon O, Ondoma O, Oliver O, Onyebuchi N (2016) Quadcopter design for payload delivery. *J Comput Commun* 04(10):1–12
- Grisso R, Alley M, Conrad H (2009) Precision farming tools: global positioning system (GPS). Communications and Marketing. College of Agriculture and Life Sciences Virginia Polytechnic Institute and State University, pp 442–503
- Hassani V, Aguiar AP, Pascoal AM et al (2009) Further results on plant parameter identification using continuous-time multiple-model adaptive estimators. In: 48th IEEE Conference on Decision and Control, held jointly with the 28th Chinese Control Conference [CDC/CCC]. pp 7261–7266. Available via <https://web.fe.up.pt/~apra/publications/cdc2009-MMAE.pdf>. Accessed 15 Dec 2021
- Hassani V, Hespanha JP, Athans M et al (2011) Stability analysis of robust multiple model adaptive control. *IFAC Proceed* 44(1):350–355. Available via <https://folk.ntnu.no/skoge/prost/proceedings/ifac11-proceedings/data/html/papers/1194.pdf>. Accessed 15 Dec 2021
- Herrera M, Gómez AP (2015) Sliding mode control: an approach to control a quadrotor. 2015 Asia-Pacific Conference on Computer Aided System Engineering, pp 314–319
- Jung HC, Kyoohyung H, Seong-Min H, Hyoun JK (2018) Toward a Secure Drone System: Flying With Real-Time Homomorphic Authenticated Encryption. *IEEE Access, Special Section on Security Analytics and Intelligence for cyber Physical System* 6:2425–2439
- Kader SA, EL Henawy AE, Oda AN (2014) Quadcopter system modeling and autopilot synthesis. *Int J Eng Res Technol*. <https://doi.org/10.17577/IJERTV3IS110007>
- Kotarski D, Beniç Z, Krzmar M (2016) Control design for unmanned aerial vehicles with four rotors. *Interdiscip Descr Complex Syst* 14(2):236–245. <https://doi.org/10.7906/index.14.2.12>
- Luo H, Niu Y, Liang Z et al (2016) Quadcopter autonomous control system based on image recognition. In: 12th World Congress on Intelligent Control and Automation [WCICA], Guilin, China, 12–15 June 2016
- Magnussen Ø, Skjønhaug KE (2011) Modeling, design and experimental study for a quadcopter system construction. M.Sc. Thesis. Department of Engineering. Faculty of Technology and Science. University of Agder
- Minh QH, Weihua Z, Lihua X (2014) L1 Adaptive control for quadrotor: design and implementation. In: International Conference on Control, Automation, Robotics and Vision Marina Bay Sands. Singapore

- Moness M, Bakr M (2015) Development and analysis of linear model representations of the quadrotor system. In: 16th International Conference on Aerospace Sciences & Aviation Technology. <https://doi.org/10.21608/ASAT.2015.22894>
- Newcome LR (2004) Unmanned Aviation: A Brief History of Unmanned Aerial Vehicles. American Institute of Aeronautics and Astronautics, Inc., 1st ed. Reston, VA: American Institute of Aeronautics and Astronautics
- Oscar Liang (2018) Quadcopter PID explained. Tutorial, 8 February. <https://oscarliang.com/quadcopter-pid-explained-tuning/>. Accessed 28 Oct 2020
- Pounds R, Mahony R, Corke P (2010) Modelling and control of a large quadrotor robot. Control Eng Pract 18(7):691–699. <https://doi.org/10.1016/j.conengprac.2010.02.008>
- Purnawan H, Mardijah, Purwanto EB (2017) Design of linear quadratic regulator [LQR] control system for flight stability of LSU-05. IOP Conf Ser. J Phys Conf Ser 890:012056. <https://doi.org/10.1088/1742-6596/890/1/012056>
- Quadcopter (2017) What is a GPS quadcopter. Available via <http://quad.phillycreative.com/category/articles/>. Accessed 29 Oct 2020
- Raafat SM, Mahmoud ZS (2018) Robust multiple model adaptive control for dynamic positioning of quadrotor helicopter system. Eng Technol J 36(12):1249–1259. <https://doi.org/10.30684/etj.36.12A.6>
- Rahemi N, Mosavi MR, Abedi AA et al (2014) Accurate solution of navigation equations in GPS receivers for very high velocities using pseudo range measurements. Adv Aerosp Eng. <https://doi.org/10.1155/2014/435891>
- Sadeghzadeh I, Abdolhosseini M, Zhang Y (2014) Payload drop application using an unmanned quadrotor helicopter based on gain-scheduled PID and model predictive control. Unmanned Syst 2(1):39–52. <https://doi.org/10.1142/S2301385014500034>
- Sattar MA, Ismail A (2017) Modeling and fuzzy logic control of a quadrotor UAV. Int Res J Eng Technol 4(08):1–5
- Schmidt MD (2011) Simulation and control of a quadrotor unmanned aerial vehicle. M.Sc. Thesis. University of Kentucky, USA
- Shahid F, Kadri MB, Jumani NA et al (2016) Dynamical modeling and control of quadrotor. Trans Mach Des 4(2):50–63. Available via <https://www.dline.info/tmd/v4n2.php>. Accessed 15 Dec 2021
- Thomas R (2010) Sliding mode controller for a quadrotor. M.Sc. Thesis, B. Engineering. Anna University, India
- Tripathi VK, Behera L, Verma N (2016) Design of sliding mode and back stepping controllers for a quadcopter. In: IEEE 39th National Systems Conference [NSC]
- Wang Z, Man Z, Cao J et al (2016) Dynamics modeling and linear control of quadcopter. In: IEEE, International Conference on Advanced Mechatronic Systems (ICAMEchS). <https://doi.org/10.1109/ICAMECHS.2016.7813499>
- Yacine D, Madjid K, Aimad A (2015) Fully decentralized fuzzy sliding mode control with chattering elimination for a quadrotor attitude. In: IEEE, 4th International Conference on Electrical Engineering, 1–6 Oct 2016
- Ziaul H (2016) Basic Concept of GPS and Its Applications. IOSR Journal of Humanities and Social Science (IOSR-JHSS) 21(3)II:31–37